Applied Energy 228 (2018) 1726–1739

Contents lists available at ScienceDirect

Applied Energy

journal homepage: www.elsevier.com/locate/apenergy

Boosting hydropower output of mega cascade reservoirs using an evolutionary algorithm with successive approximation

Yanlai Zhou[a,b], Shenglian Guo[a], Fi-John Chang[b,*], Chong-Yu Xu[a,c]

[a] State Key Laboratory of Water Resources and Hydropower Engineering Science, Wuhan University, Wuhan 430072, China
[b] Department of Bioenvironmental Systems Engineering, National Taiwan University, Taipei 10617, Taiwan, ROC
[c] Department of Geosciences, University of Oslo, 1047 Oslo, Norway

HIGHLIGHTS

- Propose successive approximation to solve curse of dimensionality raised in NSGA-II.
- NSGA-II with successive approximation optimizes 21 mega-reservoirs' joint operation.
- Lift synergy of hydropower output, flood control, water supply and CO_2 mitigation.

ARTICLE INFO

Keywords:
Hydropower output
Multi-objective optimization
Artificial Intelligence (AI)
Non-Dominated Sorting Genetic Algorithm-II (NSGA-II)
Cascade reservoirs
Yangtze River

ABSTRACT

The high complexity of multi-objective joint reservoir operation imposes challenging barriers to the pursuit of optimal hydroelectricity output. Inasmuch as multi-objective evolution optimization algorithms, including the Non-Dominated Sorting Genetic Algorithm-II (NSGA-II), are trapped in the curse of dimensionality which could not be effectively solved the multi-objective operation of more than ten reservoirs. This study proposes a methodology that integrate the NSGA-II with a successive approximation approach to optimize the hydropower output *for conquering the curse of dimensionality under the joint operation of 21 mega cascade reservoirs* located in the Upper Yangtze River Basin of China. The successive approximation approach could effectively decompose the mutually related M-dimensional problem into M individual one-dimensional problems, which ingeniously overcomes the curse of dimensionality. The proposed model is anchored with strategies of advancing impoundment timings and raising water levels of cascade reservoirs. We show that our methodology, without adding or upgrading hydraulic infrastructures, empowers the joint operation to reach 110.79 billion kW·h/year (9.8% improvement) in hydropower output, which could reduce 86.97 billion kg/year in CO_2 emission, and to provide 44.97 billion m^3/year in water supply with flood risk less than 0.016. The results suggest that our methodology can spur hydroelectricity output to support China's tactics in fulfilling the pledge of carbon emission reduction and non-fossil energy expansion to 20% by 2030.

1. Introduction

In consequence of high-speed economic growth and modern society development, China has become a big energy consumer yet a largish carbon dioxide (CO_2) emitting country in the world. China has greatly endeavored to make transit-oriented development of renewable energy systems for fulfilling the pledge of carbon emission reduction and non-fossil energy expansion to 20% by 2030 or earlier [1,2]. Thermal power, hydropower, wind power and nuclear power are the main power sources in China [3], and the annual output of each power source, as well as the ratio of individual output to the total output of the composition of these four energy sources during 2000 and 2015, are shown in Fig. 1(a). Although thermal power dominated the energy structure in China, its share showed a decreasing trend from 2000 (85.22%) to 2015 (74.24%). On the other hand, hydropower occupied over 19% of energy production in 2015, with a prominent increasing trend from 2000 (13.41%) to 2015 (19.59%). It appears that hydropower takes the lead in renewable electricity generation technology worldwide. From the perspectives of integrative operation between different renewable energies [4,5] and water resources management [6], hydropower, technically, can be commercially developed on a large scale in China at present [7]. With flexibility in electricity production

* Corresponding author.
E-mail address: changfj@ntu.edu.tw (F.-J. Chang).

https://doi.org/10.1016/j.apenergy.2018.07.078
Received 11 April 2018; Received in revised form 22 June 2018; Accepted 14 July 2018
Available online 19 July 2018

Nomenclature

Abbreviations

AI	artificial intelligence
CDR	carbon dioxide (CO_2) reduction
FR	flood risk
GHG	greenhouse gas
HO	hydropower output
IE	impoundment efficiency
NSGA-II	non-dominated sorting genetic algorithm-II
PGR	power generation risk
SOP	standard operation policy
TGR	three gorges reservoir
WS	water supply
WUB	whole upper Yangtze river basin

Indices

i	index of reservoirs, from 1 to M
t	index of time, from 1 to T·N

Parameters

$E(CO_2)$	CO_2 equivalency for hydropower generation
g	gravity acceleration
G_{max}	maximal generation in NSGA-II
M	number of reservoirs
η	dimensionless efficiency coefficient of the installation
N	number of years
N_{pop}	population size in NSGA-II
ρ	density of water
P_c	crossover probability in NSGA-II
P_m	mutation probability in NSGA-II
P_i^{min}	minimum power output of the ith reservoir
P_i^{max}	maximum power output of the ith reservoir
R_i^{min}	minimum of water release of the ith reservoir
R_i^{max}	maximum of water release of the ith reservoir
SI_i	storage corresponding to top of inactive pool in the ith reservoir
SS_i	storage corresponding to seasonal top of buffer pool in the ith reservoir
SN_i	storage corresponding to top of conservation pool in ith reservoir
Δt	time step
T	number of time-steps in a year
W_i^{min}	minimum water level of the ith reservoir
W_i^{max}	maximum water level of the ith reservoir

Variables

CDR_i	CO_2 reduction for hydropower generation in the ith reservoir
$FR(t)$	flood risk at the tth time
$FR_i(t)$	flood risk of the ith reservoir at the tth time
$H_i(t)$	head difference between the turbine intake and the last tank of the ith reservoir at the tth time
HO_i	hydropower output of the ith reservoir
$I_i(t)$	inflow of the ith reservoir at the tth time
IE_i	impoundment efficiency of the ith reservoir
$IF_i(t+1)$	stream flow of intermediate catchment between the i-1th reservoir and the ith reservoir at the $t+1$th time
$P_i(t)$	hydropower output of the ith reservoir at tth time
$PGR(t)$	power generation risk at the tth time
$PGR_i(t)$	power generation risk of the ith reservoir at the tth time
$R_i(t)$	water release of the ith reservoir at the tth time
$RT_i(t)$	water release through turbine of the ith reservoir at the tth time
$RS_i(t)$	water release through spillway of the ith reservoir at the tth time
$S_i(t)$	storage of the ith reservoir at the tth time
$SF_i(j)$	final storage of the ith reservoir in the jth year
$W_i(t)$	water level of the ith reservoir at the tth time
WS_i	water supply of the ith reservoir

and supply, hydropower development brings substantial benefits to energy economy [8,9], energy safety [10], climate change mitigation [11,12] and GHG emission reduction [13,14].

The installed hydropower capacity of China reached 320 GW by the end of 2016, which was attributed to the fast development of hydropower resources and the intensive construction of power grids during the past three decades [15]. Delivering an annual hydropower output of 1130 billion kWh, China ranked first with a share of 32% in global hydropower generation by 2016 [16]. Hydropower resources are concentrated mainly in south-western China while electricity loads occur mainly around the Yangtze River Delta and the Pearl River Delta [17]. With a total length of 6300 km and terrain elevation ranging between 10 m and 7213 m, the Yangtze River has an average annual runoff of 995.8 billion m^3 and a drainage area of 1.80 million km^2. Being credited to the merits in nature, the Yangtze River Basin possesses the largest water and hydropower resources in China. A total of 249 mega reservoirs (reservoir capacity $\geq$100 million m^3) and 1327 medium-scale reservoirs (10 million $m^3 \leq$ reservoir capacity $<$ 100 million m^3) accompanied with hydropower plants were built and operated in this basin during the last two decades, and their total hydropower output accounted for over 30% of the installed hydropower capacity in China [18]. To date, the number of reservoirs for joint operation during flood seasons is usually less than ten [15–17]. The management of cascade reservoir operation in consideration of multiple perspectives is highly complex and usually involves multi-objective [19], large-scale, trans-basin [20], trans-province, and trans-region issues [21,22]. Major barriers also lie in the high dimensionality of the whole system and the very large number of variables required for modelling joint operation [22]. Concerns also arise on the costly and time-consuming construction of new dams and/or hydropower plants. Besides, environmental impact assessment may prohibit such construction. Therefore, it is essential to conduct in-depth research with state-of-the-art techniques to conquer challenges encountered in such awkward situation of join cascade reservoir operation for effectively promoting the synergies among hydropower generation, flood control, water utilization and CO_2 emission reduction.

Due to the complexity of the joint operation of cascade reservoirs, plenty of optimization algorithms involving mathematical programming methods and artificial intelligence algorithms have been introduced and applied to reservoir operation and management. The mathematical programming methods, for instance non-linear programming (NLP), dynamic programming (DP) and stochastic dynamic programming (SDP), are storage-consuming and computationally inefficient. These bottlenecks caused by high-dimensionality are partially overcome by some approximation algorithms based on DP, such as progressive optimality algorithm (POA) [23] and dynamic programming successive approximation (DPSA) [24–26]. However, on the whole, these methods with inherent drawbacks have been primarily applied to single-objective optimization operation of cascade reservoirs because the curse of dimensionality has not been totally solved. Also,

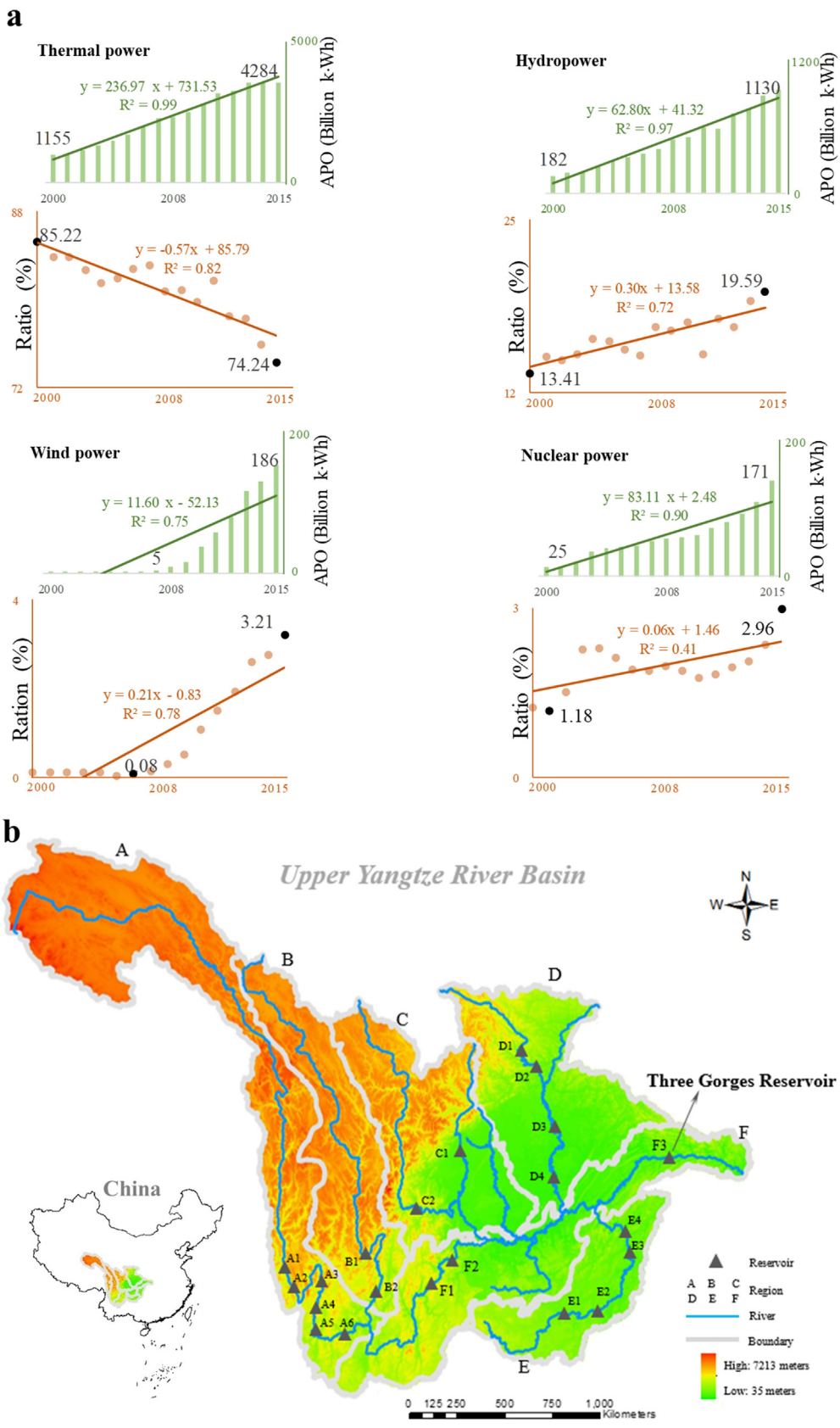

Fig. 1. Statistics of main power sources in China and the investigative area of this study. a. Annual power output (APO) and the ratio of individual power output to the total output of the four types of energy in China during 2000 and 2015 are presented, respectively. b. Spatial distribution of 21 cascade reservoirs in the Upper Yangtze River Basin.

there still are limitations arising from the complex simulation models in the form of spatial-temporal hydraulic and electricity connections between high-dimensional cascade reservoirs. Artificial intelligence algorithms, such as genetic algorithm (GA), non-dominated sorting genetic algorithm-II (NSGA-II), particle swarm optimization (PSO), multi-objective particle swarm optimization (MOPSO), differential evolution (DE) and multi-objective differential evolution (MODE) algorithm, can be adequately integrated with simulation models to significantly lift the performance of single-objective and multi-objective optimization operation, respectively. However, their applicability is somewhat limited by computational difficulties that arise in high-dimensional problems. For instance, the number of cascade reservoirs in single-objective optimization using GA [27], PSO [28] and DE [29] is less than ten while the number of cascade reservoirs in multi-objective optimization using NSGA-II [30,31], MOPSO [32] and MODE [33] is less than five. Inasmuch as multi-objective evolution optimization algorithms, including the standard NSGA-II proposed by Deb et al. [34], are trapped in the curse of dimensionality, where global optimum is difficult to obtain. It is highly challenging and complex to model and/or optimize the joint operation of more than ten reservoirs [22,35]. Hence, to pinpoint the current and prospective mega cascade reservoir systems (more than ten cascade reservoirs), the key scientific measure to tackle such high-dimensional problems is to propose an effective and efficient optimization method so as to address multi-objective optimization and curse of dimensionality. To obtain the solution of a high-dimensional cascade reservoir optimization model, a novel methodology that integrates an evolutionary algorithm with successive approximation is presented in this study based on the nature of the standard NSGA-II and a successive approximation approach.

This study was explored with two main foci: proposing two pre-set strategies that advance impoundment operation timing and lift reservoir water level for multi-objective impoundment operation of cascade reservoirs; and fusing the non-dominated sorting genetic algorithm-II (NSGA-II) with a successive approximation approach for coping with the curse of dimensionality caused by high dimensionality and a great number of variables required for modelling the joint operation of

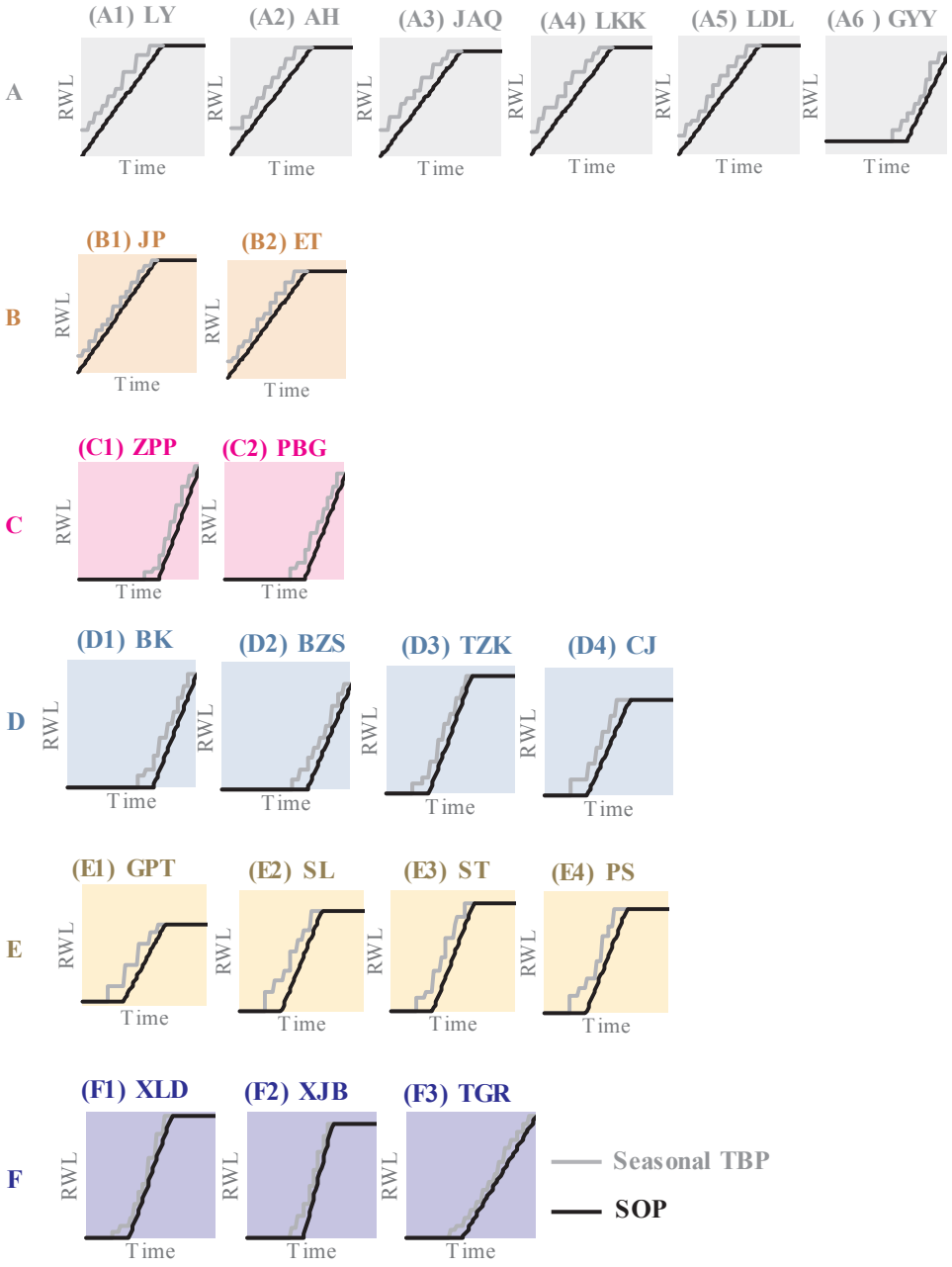

Fig. 2. Operation curves of reservoir impoundment. SOP denotes the standard operation policy; TBP denotes the top of buffer pool; and RWL denotes the reservoir water level. The 21 cascade reservoirs are located in six regions (A–F) of the Upper Yangtze River Basin. Reservoirs in each region: Region A: Reservoirs LY (Li-Yuan); AH (A-Hai); JAQ (Jin-An-Qiao); LKK (Long-Kai-Kou); LDL (Lu-Di-La); and GYY (Guan-Yin-Yan); Region B: Reservoirs JP (Jin-Ping); and ET (Er-Tan); Region C: Reservoirs ZPP (Zi-Ping-Pu); and PBG (Pu-Bu-Gou); Region D: Reservoirs BK (Bi-Kou); BZS (Bao-Zhu-Si); TZK (Ting-Zi-Kou); and CJ (Cao-Jie); Region E: Reservoirs GPT (Gou-Pi-Tan); SL (Si-Lin, ST); ST (Sha-Tuo) and PS (Peng-Shui); Region F: Reservoirs XLD (Xi-Luo-Du); XJB (Xiang-Jia-Ba); and TGR (Three Gorges Reservoir, the largest reservoir in the world to date).

mega cascade reservoirs. In this study we, under current hydraulic infrastructures, propose to model this highly complex issue for significantly spurring hydroelectricity output in consideration of water utilization efficiency, flood control and CO_2 emission mitigation. These issues were examined via a detailed case study on the 21 mega cascade reservoir in the Upper Yangtze River Basin of China (Fig. 1(b)). The remainder of the study is structured as follows: Section 2 introduces the study area and materials; Section 3 presents the methods used in the analysis; Section 4 presents and discusses the results; and conclusions are then drawn in Section 5.

2. Study area and materials

The Yangtze River (i.e., Chang-Jiang) is the longest river in China, and many farm lands and industrial areas are located along the river. Due to complex mountainous topography and subtropical climate, floods are commonly induced by heavy rainfalls (200–800 mm) within 24 h in the Yangtze River Basin, and thus cause high flood risks. A series of large reservoirs are located in this basin for multiple purposes in recent decades. Among them, the Three Gorges Reservoir (TGR) is the largest reservoir in the world and implements the largest hydroelectric project to date, which not only can generate approximately 22.50 GW (GW) of hydropower (i.e. installed capacity) but also protect millions of downstream residents from flood hazards. To promote water resources utilization and renewable hydropower generation, 21 mega cascade reservoirs in the Upper Yangtze River Basin (Fig. 1(b)) have operated jointly to achieve a total reservoir storage of 109.76 billion m^3 (34.2 billion m^3 for flood control) and a total installed hydropower capacity of 78.65 GW.

In Fig. 2, the current rules (i.e. the standard operation policy (SOP)) for the joint operation of 21 cascade reservoirs consist of: (1) the reservoir storage level would be linearly raised from the annual top of buffer pool at the starting time of impoundment to the top of conservation pool at the end of flood seasons; (2) the initial impoundment operation would be activated no earlier than August 1st (Table 1); and (3) the operation of cascade reservoirs should be implemented between August 1st and October 31st according to geological distributions of reservoirs along the Yangtze River (e.g. reservoirs in Region D start on August 1st, but reservoirs in Region E start on September 1st, see Table 1) [36]. Data applied in this study consist of a total of 119,784 datasets (= 21 reservoirs * 92 days * 62 years) collected in flood seasons (August 1st - October 31st, 92 days) during 1955 and 2016 (62 years).

3. Methods

Because the intrinsic nature of hydrology is nonlinear and uncertain, a linear operation curve like the Standard Operation Policy (SOP, see Fig. 3(a)) used in China may not satisfactorily compromise the risks between flood control and hydropower generation. We intend to solve this problem, and the research flowchart of this study is shown in Fig. 3. We first propose two pre-set operation strategies to aptly construct the constraints of reservoir water level for impoundment operation (Fig. 3(a)). Then, the non-dominated sorting genetic algorithm-II (NSGA-II) with successive approximation approach is developed to search the optimal multi-objective impoundment operation of 21 cascade reservoirs. The Pareto frontiers obtained from the NSGA-II are generated to reflect the trade-off risks of flood control and hydropower generation. The details of the methods used in this study are

Table 1
Impoundment timings, water levels and basic statistics of 21 cascade reservoirs in the six regions (A–F) of the Upper Yangtze River Basin (WUB).

Region	Reservoir[a]	Initial reservoir impoundment timing		Final reservoir impoundment timing	Annual top of buffer pool[c]	Top of conservation pool	Total storage capacity	Storage capacity for flood control	Installed hydropower capacity
		(SOP[b])	(NSGA-II)	(SOP, NSGA-II)	(m)	(m)	(Billion m^3)	(Billion m^3)	(GW)
Region A[f] (Jin-Sha River)	(A1) LY	Aug. 1st	*[d] Aug.1st	Sep. 30th	1605	1618	0.81	0.17	2.40
	(A2) AH	Aug. 1st	*Aug.1st	Sep. 30th	1493.3	1504	0.89	0.22	2.00
	(A3) JAQ	Aug. 1st	*Aug.1st	Sep. 30th	1410	1418	0.91	0.16	2.40
	(A4) LKK	Aug. 1st	*Aug.1st	Sep. 30th	1289	1298	0.56	0.13	1.80
	(A5) LDL	Aug. 1st	*Aug.1st	Sep. 30th	1212	1223	1.72	0.56	2.16
	(A6) GYY	Oct. 1st	#[c] Sep.10th	Oct. 31st	1128.8	1134	2.25	0.25	3.00
Region B (Ya-Long River)	(B1) JP	Aug. 1st	*Aug.1st	Sep. 30th	1859	1880	7.99	1.60	3.60
	(B2) ET	Aug. 1st	*Aug.1st	Sep. 30th	1190	1200	5.80	0.90	3.30
Region C (Min River)	(C1) ZPP	Oct. 1st	#Sep.10th	Oct. 31st	850	877	1.11	0.17	0.76
	(C2) PBG	Oct. 1st	#Sep.10th	Oct. 31st	841	850	5.33	0.73	3.60
Region D (Jia-Ling River)	(D1) BK	Oct. 1st	#Sep.10th	Oct. 31st	695	704	0.22	0.10	0.30
	(D2) BZS	Oct. 1st	#Sep.10th	Oct. 31st	583	588	2.55	0.28	0.70
	(D3) TZK	Sep. 1st	#Aug. 20th	Sep. 30th	447	458	4.07	1.44	1.10
	(D4) CJ	Sep. 1st	#Aug. 20th	Sep. 30th	200	203	2.22	0.20	0.50
Region E (Wu River)	(E1) GPT	Sep. 1st	#Aug. 20th	Sep. 30th	628.1	630	6.45	0.20	3.00
	(E2) SL	Sep. 1st	#Aug. 20th	Sep. 30th	435	440	1.59	0.18	1.05
	(E3) ST	Sep. 1st	#Aug. 20th	Sep. 30th	357	365	0.92	0.21	1.12
	(E4) PS	Sep. 1st	#Aug. 20th	Sep. 30th	287	293	1.47	0.23	1.75
Region F (XLD-XJB-TGR)	(F1) XLD	Sep. 1st	#Aug. 25th	Sep. 30th	560	600	12.67	4.65	13.86
	(F2) XJB	Sep. 10th	#Aug. 25th	Sep. 30th	370	380	5.16	0.90	7.75
	(F3) TGR	Sep. 10th	#Aug. 25th	Oct. 31st	145	175	45.07	22.15	22.50

[a] Operation period starting from 1st of August to 31st of October.
[b] Standard operation policy.
[c] Set as the initial reservoir water level in reservoir operation.
[d] Implement the strategy of raising reservoir water level.
[e] Implement the strategies of advancing reservoir impoundment timing and raising reservoir water level.
[f] Reservoirs of each region: Region A: Reservoirs LY (Li-Yuan); AH (A-Hai); JAQ (Jin-An-Qiao); LKK (Long-Kai-Kou); LDL (Lu-Di-La); and GYY (Guan-Yin-Yan); Region B: Reservoirs JP (Jin-Ping); and ET (Er-Tan); Region C: Reservoirs ZPP (Zi-Ping-Pu); and PBG (Pu-Bu-Gou); Region D: Reservoirs BK (Bi-Kou); BZS (Bao-Zhu-Si); TZK (Ting-Zi-Kou); and CJ (Cao-Jie); Region E: Reservoirs GPT (Gou-Pi-Tan); SL (Si-Lin, ST); ST (Sha-Tuo); and PS (Peng-Shui); Region F: Reservoirs XLD (Xi-Luo-Du); XJB (Xiang-Jia-Ba); and TGR (Three Gorges Reservoir, the largest reservoir in the world to date).

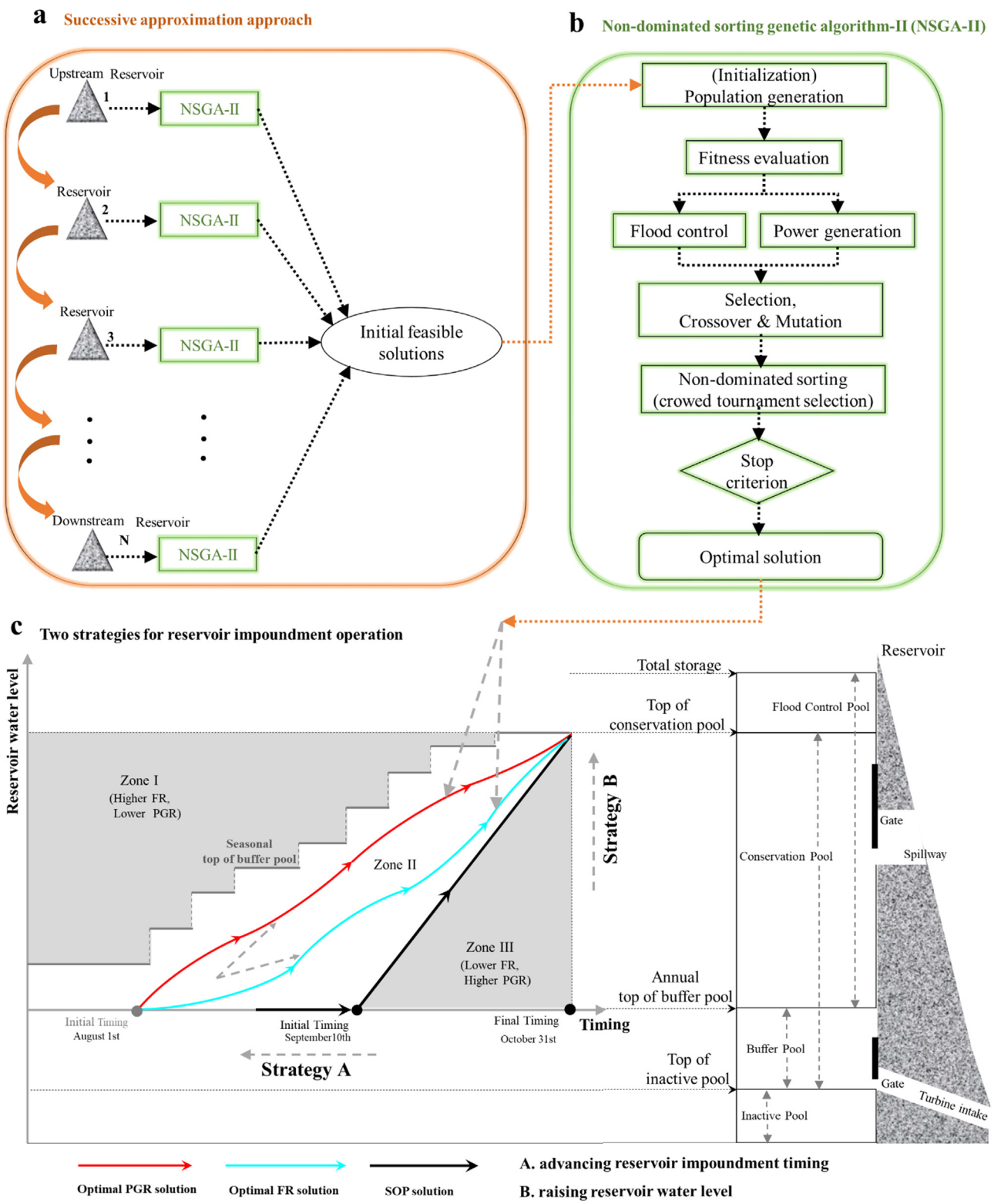

Fig. 3. Solutions to reservoir impoundment operation. (a) Successive approximation approach. (b) Non-dominated sorting algorithm-II (NSGA-II). (c) Two strategies for reservoir impoundment operation. FR denotes flood risk; PGR denotes hydropower generation risk; SOP denotes the standard operation policy; the top of buffer pool is set as the initial reservoir water level; and the reservoir impoundment operation curve is divided into three zones (I, II and III) by reservoir parameters (i.e. annual top of buffer pool, seasonal top of buffer pool, top of conservation pool, SOP operation curve, as well as initial and final timings of reservoir impoundment operation).

given as follows.

3.1. Multi-objective joint operation of cascade reservoirs

The multi-objective joint operation of cascade reservoirs is modelled with the aim of synergistically minimizing the trade-offs in risks

between flood control and hydropower generation of the river-basin system. The flood risk (FR) is formulated by the ratio of flood control capacity loss to total flood control capacity. The power generation risk (PGR) is estimated by the ratio of hydropower generation shortage (occurs when power output is less than installed power output) to potential power generation amount, because the power output of a hydraulic turbine is restrained between guaranteed (minimum) power output and installed (maximum) power output [40]. A sketch of the variables used to define objective functions and constraints is presented in Fig. 4. The multi-objective optimization model is formulated as follows:

3.1.1. Objective functions

Objective 1: minimizing flood risk

$$\mathrm{FR} = \min\{\max\{\mathrm{FR}(t)\}\}, \quad (0 < t \leqslant \mathrm{T}\cdot\mathrm{N}) \tag{1a}$$

$$\mathrm{FR}(t) = \frac{\sum_{i=1}^{\mathrm{M}} (\mathrm{S}_i(t) - \mathrm{SS}_i)}{\sum_{i=1}^{\mathrm{M}} (\mathrm{SN}_i - \mathrm{SS}_i)} \tag{1b}$$

$$\mathrm{FR}_i(t) = \frac{\mathrm{S}_i(t) - \mathrm{SS}_i}{\mathrm{SN}_i - \mathrm{SS}_i} \tag{1c}$$

where FR is the flood risk; FR(t) is the flood risk at the tth time; FR_i(t) is the flood risk of the ith reservoir at the tth time; T is the number of time-steps in a year; N is the number of years; M is the number of reservoirs; $\mathrm{S}_i(t)$ is the storage of the ith reservoir at the tth time; SS_i is the storage corresponding to the seasonal top of buffer pool in the ith reservoir; and SN_i is the storage corresponding to the top of conservation pool in the ith reservoir.

Objective 2: minimizing power generation risk (i.e. maximizing hydropower output)

$$\mathrm{PGR} = \min\{\max\{\mathrm{PGR}(t)\}\}, \quad (0 < t \leqslant \mathrm{T}\cdot\mathrm{N}) \tag{2a}$$

$$\mathrm{PGR}(t) = \frac{\sum_{i=1}^{\mathrm{M}} (\mathrm{P}_i^{\max} - \mathrm{P}_i(t))}{\sum_{i=1}^{\mathrm{M}} (\mathrm{P}_i^{\max} - \mathrm{P}_i^{\min})} \tag{2b}$$

$$\mathrm{PGR}_i(t) = \frac{\mathrm{P}_i^{\max} - \mathrm{P}_i(t)}{\mathrm{P}_i^{\max} - \mathrm{P}_i^{\min}} \tag{2c}$$

where PGR is the hydropower generation risk; PGR(t) is the hydropower generation risk at the tth time; $\mathrm{PGR}_i(t)$ is the hydropower generation risk of the ith reservoir at the tth time; $\mathrm{P}_i(t)$ is the hydropower output of the ith reservoir at tth time; $\mathrm{P}_i^{\max}$ is the maximum hydropower output of the ith reservoir; and $\mathrm{P}_i^{\min}$ is the minimum hydropower output of the ith reservoir.

3.1.2. Constraints

Reservoir operation should obey physical constraints, such as the water balance equation, the hydraulic connection equation, the feasible boundary of water release, hydropower output and the reservoir water level. The mathematical formulations of these constraints are given as follows.

$$\mathrm{S}_i(t+1) = \mathrm{S}_i(t) + \left(\frac{\mathrm{I}_i(t+1) + I_i(t)}{2} - \frac{\mathrm{R}_i(t+1) + R_i(t)}{2}\right)\cdot\Delta\mathrm{t} \tag{3}$$

$$\mathrm{I}_i(t+1) = \mathrm{R}_{i-1}(t+1) + \mathrm{IF}_i(\mathrm{t}+1) \tag{4}$$

$$\mathrm{R}_i(t) = \mathrm{RT}_i(t) + \mathrm{RS}_i \tag{5a}$$

$$\mathrm{R}_i^{\min} \leqslant \mathrm{R}_i(t) \leqslant \mathrm{R}_i^{\max} \tag{5b}$$

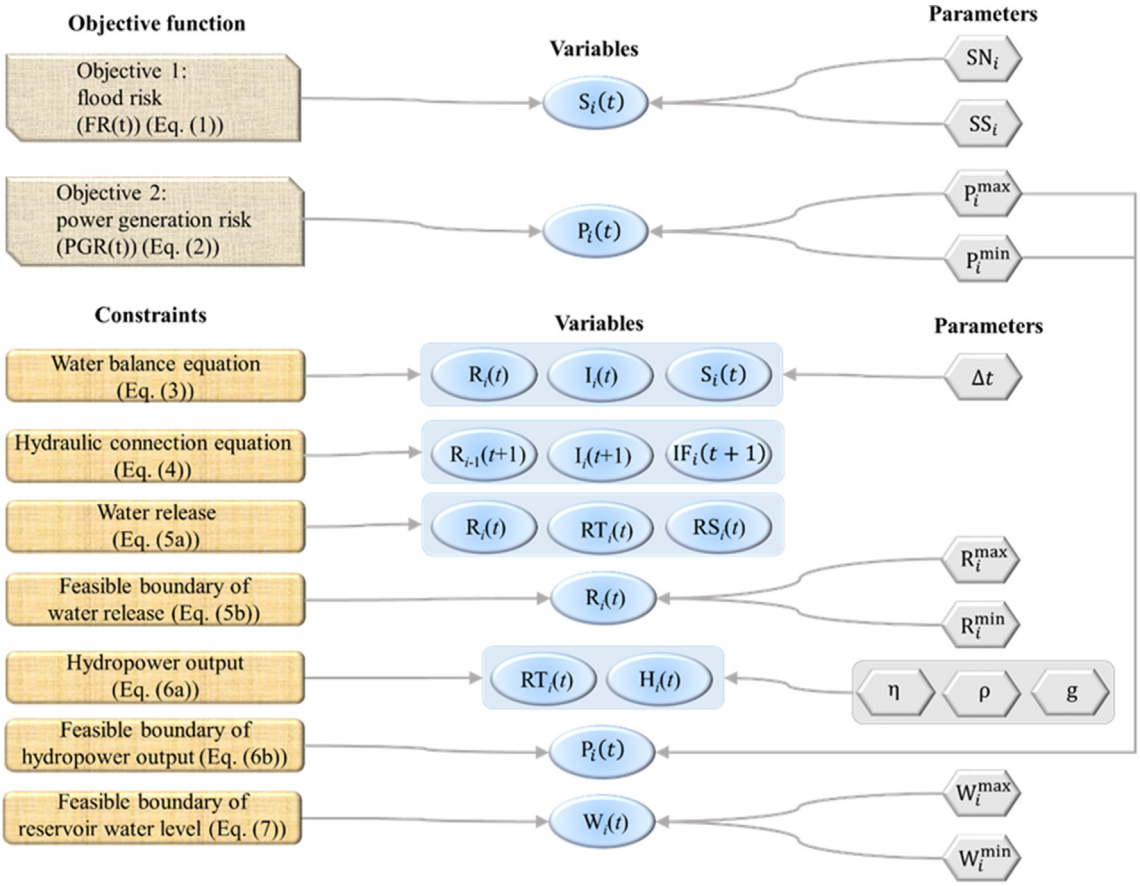

Fig. 4. Sketch of the variables used to define objective functions and constraints.

$$P_i(t) = \eta \cdot \rho \cdot g \cdot RT_i(t) \cdot H_i(t) \quad (6a)$$

$$P_i^{min} \leqslant P_i(t) \leqslant P_i^{max} \quad (6b)$$

$$W_i^{min} \leqslant W_i(t) \leqslant W_i^{max} \quad (7)$$

where $I_i(t)$ and $R_i(t)$ are the inflow and water release of the ith reservoir at the tth time, respectively. $IF_i(t+1)$ is the stream flow of the intermediate catchment between the i-1th reservoir and the ith reservoir at the $t+1$th time. $RT_i(t)$ and $RS_i(t)$ are the water release through turbine and spillway of the ith reservoir at the tth time, respectively. R_i^{min} and R_i^{max} are the minimum and maximum of water release of the ith reservoir, respectively. $P_i(t)$ is the output power of the ith reservoir at the tth time. η is the dimensionless efficiency coefficient of the installation. ρ is the density of water. g is the gravity acceleration. $H_i(t)$ is the head difference between the turbine intake and the last tank of the ith reservoir at the tth time. P_i^{min} and P_i^{max} are the minimum and maximum power output of the ith reservoir, respectively. $W_i(t)$ is the water level of the ith reservoir at the tth time. W_i^{min} and W_i^{max} are the minimum and maximum water level of the ith reservoir, respectively. The variables of above equations are non-negative.

In this study, the W_i^{min} and W_i^{max} are equal to annual top of buffer pool and seasonal top of buffer pool, respectively. Eqs. (3) and (4) are the water balance equation and hydraulic connection equation, respectively. Eqs. (5)–(7) show the constraints of water release, power output and reservoir water level, respectively.

3.2. NSGA-II with a successive approximation approach

The multi-objective optimization operation of M (M = 21 in our case) mega cascade reservoirs in flood seasons is typically a highly non-convex nonlinear function characterized by many constraints, where the variables and equations of the model could be discontinuous and/or non-differentiable with many local minima. The objective functions of flood risk (Eq. (1)) and hydropower generation risk (Eq. (2)) are the statistic characteristics of simulation results, while the constraints are a set of strong restraints constituted by the hydraulic and electricity connections between high-dimensional cascade reservoirs. The non-dominated sorting genetic algorithm-II (NSGA-II) proposed by Deb et al. [34] has the ability to search a diverse set of Pareto Frontiers. NSGA-II can be easily integrated with simulation models to improve the performance of non-linear multi-objective optimization. Although the NSGA-II has been found quite successful in tackling a wide variety of reservoir optimization operation and water resources management problems [30,37–41], it, similar to other evolutionary intelligent algorithms, has a drawback of the curse of dimensionality, especially in complex high-dimensional optimization problems. The number of reservoirs for joint operation during flood seasons is usually less than ten due to the curse of dimensionality mentioned previously. Because the numbers of decision variables and constraints in this river system are huge and they are closely interacted and notoriously influenced, how to search the optimal solution to this meta complex nonlinear system became a great challenge. Being credited to the recent development of computers with high-speed computation ability and huge storage capacity, this complex high-dimensional problem can be managed much more efficiently and satisfactorily. In general, the standard NSGA-II creases a new solution using its antecedent solution (previous best solution) with crossover and mutation operators. For the proposed hybrid evolutionary algorithm with successive approximation, operation policies are first produced by the standard NSGA-II, and then the joint reservoir operation is optimized successively by incorporating a successive approximation approach into the NSGA-II. That is to say, the NSGA-II coupled with a successive approximation approach can reduce the dimension of decision variables through progressively implementing a series of optimization procedure associated with each cascade reservoir from upstream to downstream, and thus would improve the capability of jumping out of local minima and searching for global optimum.

The proposed hybrid evolutionary algorithm (NSGA-II) with a successive approximation approach implements the following computation steps.

Step 1: Initialize feasible solutions of a population P_0 of size N_{pop} based on the standard NSGA-II procedure (Fig. 3(a)) for every reservoir and evaluate fitness values; implement the fast non-dominated sorting to divide the population into different ranks; and calculate crowding distances of the population.
Step 2: Implement the crowded tournament selection operator to choose chromosomes with a higher fitness value (i.e., elitism preservation strategy) for producing the offspring of the next generation in the gene pool; implement the crossover operator with probability (P_c) to re-combine two parent chromosomes into new offspring chromosomes; and implement mutation operator with probability (P_m) for maintaining genetic diversity in the population. Three genetic operators are utilized to generate an offspring population Q_0 of size N_{pop}.
Step 3: For every generation t, evaluate the fitness values of Q_t; combine Q_{t-1} and Q_t into an intermediate population P_t of size $2N_{pop}$; implement the fast non-dominated sorting to divide this combined population into different ranks; and compute crowding distances of the population.
Step 4: Select a new parent population P_{t+1} of size N_{pop} from P_t using the crowded tournament selection; generate an offspring population Q_{t+1} through crossover and mutation operators; and evaluate their fitness values.
Step 5: Terminate the computation based on stop criteria by evaluating the solutions through Steps 2–4. If the iteration number is less than the maximal generation (G_{max}), then repeat Steps 2–5. Otherwise, output the best solution set ($S_{best,0}$) as the initial input of the NSGA-II coupled with a successive approximation approach.
Step 6: Implement the successive approximation approach. Regenerate the decision variables of the 1st reservoir in the upper river basin to obtain the new best solution set ($S_{best,1}$) as well as the corresponding fitness according to Steps 2 and 3 while the other decision variables of the 2nd – Mth reservoirs remain unchanged. If the fitness of the new solution set ($S_{best,1}$) is better than that of the previous best solution set ($S_{best,0}$), then $S_{best,0}$ is replaced by $S_{best,1}$.
Step 7: Select the next reservoir to be optimized and update the solution set. The successive approximation approach is used to successively generate the initial feasible solutions for each cascade reservoir located from upstream to downstream (Fig. 3(b)). In other words, the mutually related M-dimensional (M = 21 cascade reservoirs) initial feasible solutions will be effectively decomposed into M individual one-dimensional initial feasible solutions, which adequately overcomes the curse of dimensionality.
Step 8: Repeat Step 7 until the whole cascade reservoirs system has been optimized progressively to obtain the multi-objective optimal solutions (Fig. 3(c)).

In our case, this NSGA-II model is driven by a total of 119,784 datasets (=21 reservoirs * 92 days * 62 years), which means we have 119,784 decision variables and 479,136 constraints (=4 equations * 119,784 decision variables). The use of the proposed successive approximation approach will effectively reduce the numbers of decision variables to 5704 (=92 * 62) and constraints to 22,816 (=4 * 92 * 62), respectively, where the 21-dimensional initial feasible solutions could be decomposed into 21 one-dimensional initial feasible solutions. After implementing an intensive trial-and-error procedure (e.g. sought for a large number of initial feasible solutions to satisfy more than ten thousand constraints), the parameters used in running the NSGA-II for searching converged solutions were set as: population size N_{pop} = 1000; G_{max} = 500; P_c = 0.9; and P_m = 0.1. The non-dominated solutions can provide decision makers and stakeholders with an

opportunity to evaluate and pre-experience the consequences of various alternatives between the two objectives.

3.3. Evaluation indicator

Considering the complex water-energy nexus of cascade reservoir operation, one must not rely solely on one single criterion when evaluating the contribution of multi-objective reservoir operation to sustainable hydropower development. The six evaluation indicators, i.e. flood risk (Eq. (1)), power generation risk (Eq. (2)), hydropower output, reservoir impoundment efficiency, water supply and CO_2 equivalency, were applied to making a comprehensive assessment on the performance of the optimal reservoir operation solutions. The latter four indicators are described as follows.

Annual average hydropower output (HO)

$$HO = \sum_{i=1}^{M} HO_i \tag{8a}$$

$$HO_i = \frac{1}{N} \sum_{i=1}^{T \cdot N} P_i(t) \cdot \Delta t \tag{8b}$$

where HO is the hydropower output; HO_i is the hydropower output of the ith reservoir; M is the number of reservoirs; and Δt is the time step.

Annual average reservoir impoundment efficiency (IE)

$$IE = \frac{1}{N} \sum_{j=1}^{N} \frac{\sum_{i=1}^{M} (SF_i(j) - SI_i)}{\sum_{i=1}^{M} (SN_i - SI_i)} \times 100\% \tag{9a}$$

$$IE_i = \frac{1}{N} \sum_{j=1}^{N} \frac{SF_i(j) - SI_i}{SN_i - SI_i} \times 100\% \tag{9b}$$

where IE is the impoundment efficiency; IE_i is the impoundment efficiency of the ith reservoir; $SF_i(j)$ is the final storage of the ith reservoir in the jth year; and SI_i is the storage corresponding to the top of inactive pool in the ith reservoir.

Annual average water supply (WS)

$$WS = um_{i=1}^{M} WS_i \tag{10a}$$

$$WS_i = \frac{1}{N} \sum_{j=1}^{N} (SF_i(j) - SI_i) \tag{10b}$$

where WS is the water supply; and WS_i is the water supply of the ith reservoir.

Annual average carbon dioxide (CO2) reduction (CDR)

$$CDR = \sum_{i=1}^{M} CDR_i \tag{11a}$$

$$CDR_i = HO_i \cdot E(CO_2) \tag{11b}$$

where $E(CO_2)$ is the CO_2 equivalency for hydropower generation; CDR is the CO_2 reduction for hydropower generation; and CDR_i is the CO_2 reduction for hydropower generation in the ith reservoir.

4. Results and discussion

An AI-based optimization approach triggering a new niche in spurring hydropower output under existing hydraulic infrastructures is

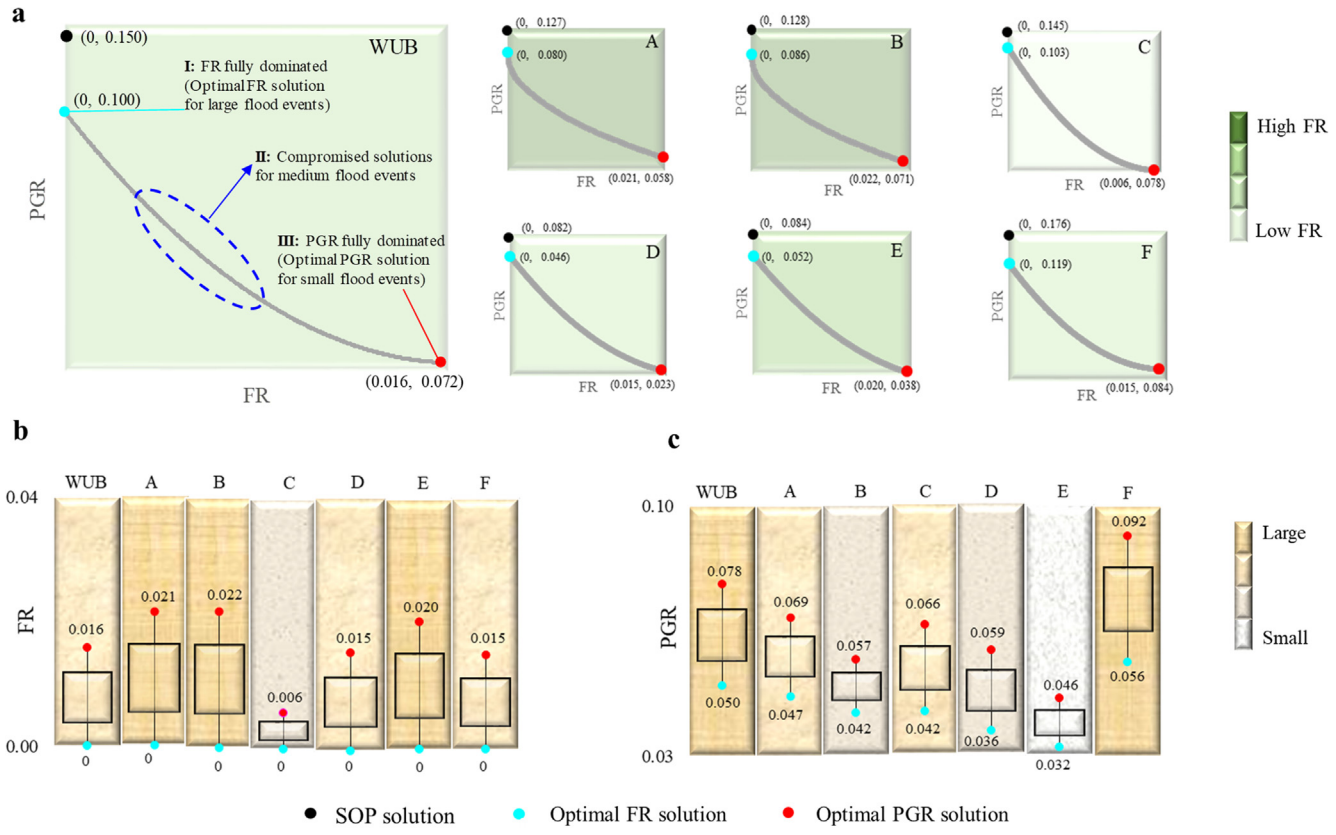

Fig. 5. Illustration of the SOP solution and the optimal solutions of the NSGA-II. (a) NSGA-II Pareto Frontiers between flood risk (FR) and hydropower generation risk (PGR). (b) Increase of FR = $FR_{NSGA\text{-}II} - FR_{SOP}$. (c) Decrease of PGR = $PGR_{SOP} - PGR_{NSGA\text{-}II}$. The comparative results of the joint operation of 21 cascade reservoirs obtained from the SOP and the NSGA-II are illustrated according to the whole Upper Yangtze River Basin (WUB) and the six regions (A–F), respectively.

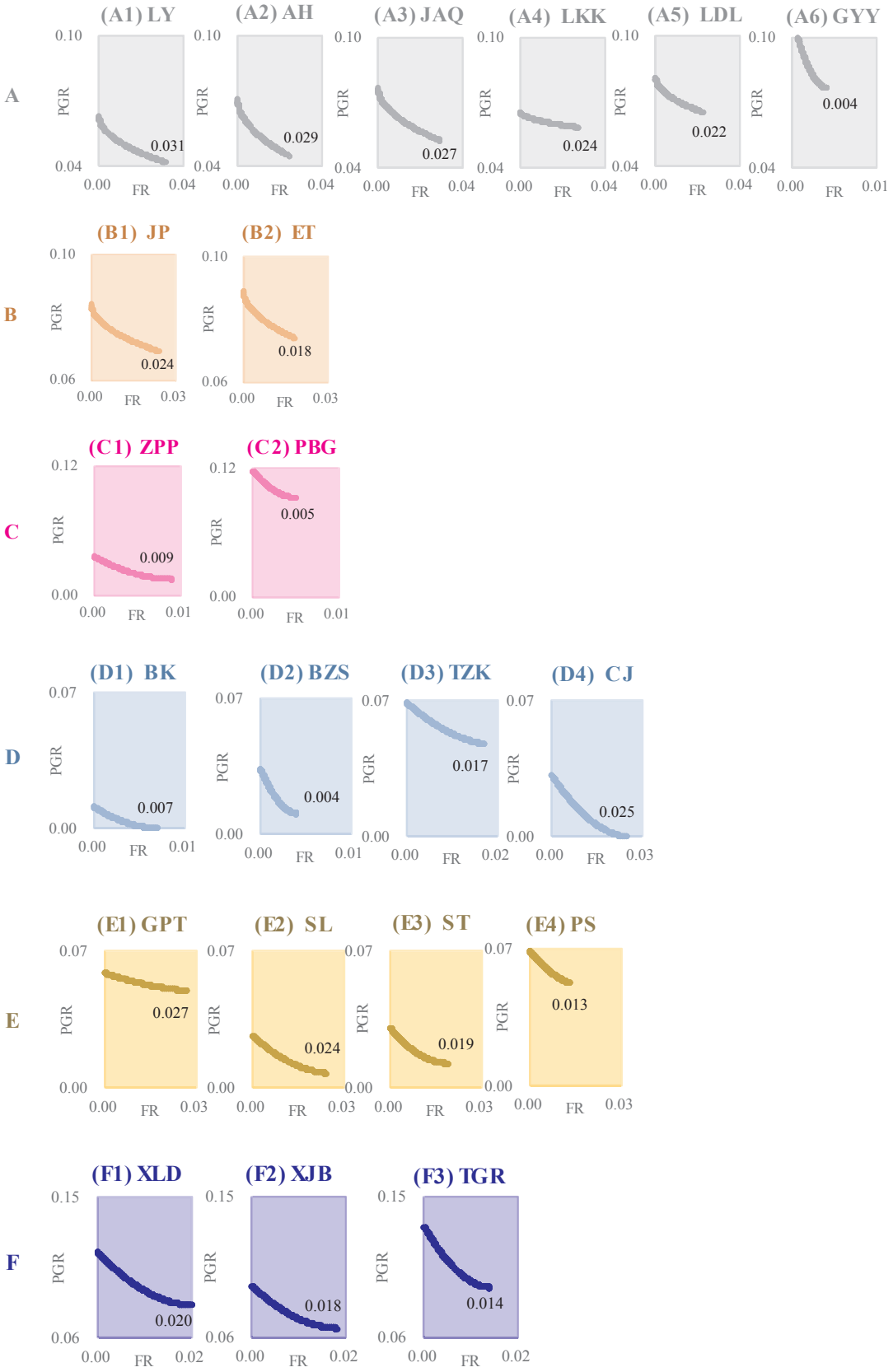

Fig. 6. Pareto Frontiers between flood risk (FR) and power generation risk (PGR). The illustration is made for 21 cascade reservoirs in six regions (A-F) of the whole Upper Yangtze River Basin.

explored in this study. We comprehensively investigate the behavior revealed in the joint operation of the top 21 cascade reservoirs with total reservoir storage exceeding 109.76 billion m^3 in the whole Upper Yangtze River Basin (WUB) of China (Fig. 1(b), Table 1). Prior to construction of the optimization model, we suggest strategies of earlier timings of initial impoundment and higher water levels (water head for hydropower generation) of reservoirs after cross-examining the climatic and hydrological data of this study area (see Table 1). These two operational strategies will pave the way for boosting hydropower output. Based on the two strategies, we next develop an optimization model for the joint operation of 21 mega cascade reservoirs in flood seasons, targeting hydropower generation while considering flood control, water utilization and CO_2 emission reduction. This model is driven by a total of 119,784 datasets (=21 reservoirs * 92 days * 62 years), where these massive high-dimensional data consist of the initial and final reservoir impoundment timings, annual and seasonal tops of the buffer pools of reservoirs, and daily reservoir inflow series collected in flood seasons (August 1st–October 31st, 92 days) during 1955 and 2016 (62 years) (Table 1 and Fig. 2). It is noted that the very complex nonlinear operation system with huge numbers of decision variables (119,784) and constraints (479,136 = 4 equations × 119,784) in our case can be tackled by the proposed methodology (shown in Fig. 3). The results are presented and discussed in details, shown below.

4.1. Behavior assessment between hydropower generation and flood control

In this study, the NSGA-II is implemented with two objectives: minimizing flood risk (FR) and minimizing hydropower generation risk (PGR) (i.e. maximizing hydropower output; refer to Eqs. (1a) and (2a) of Section 3). Each of the Pareto Frontiers obtained from the NSGA-II represents an optimal solution, where no objective can be improved without sacrificing at least one other objective. The SOP of reservoirs serves as the benchmark in this study. Fig. 5(a) visualizes the SOP solutions and the widely and distinctly distributed Pareto Frontiers obtained from the NSGA-II for the WUB and Regions A–F, respectively. The results show that the NSGA-II not only produces the best solution to each objective but supplies a large number of optimal solutions compromised between both objectives, which means the Pareto Frontier solutions can adjustably counterbalance the risks between flood control operation and hydropower generation simultaneously. That is to say, more operational alternatives are available to decision makers. Besides, the NSGA-II always produces much smaller hydropower generation risks than the SOP when there is no flood risk (flood risk = 0). For a very large watershed like the Yangtze River Basin (1.8 million km^2), the effect of a single flood event on reservoir operation in various regions could be very different. From the perspective of the optimization of flood control operation, the solutions of the Pareto Frontiers can be adaptive to different magnitudes of flood events: the minimum flood risk solution (Point I of WUB in Fig. 5(a)) is suitable for managing large-scale flood events; the minimum hydropower generation risk solution (Point III of WUB in Fig. 5(a)) is suitable for managing small-scale flood events; and the compromised solutions are suitable for managing medium-scale flood events.

Fig. 5(b) and (c) summarizes the differences in flood risk and hydropower generation risk between the SOP solution and the optimal solutions (1000 in our case) of the NSGA-II in the WUB and Regions A-F, respectively. From Fig. 5(b), the increase ($=FR_{NSGA\text{-}II} - FR_{SOP}$) of flood risk spans between 0 and 0.016 for the WUB. In Regions A, B, E and F (Fig. 6), we have two important findings. The first finding is that the maximum flood risk decreases with the elevations of reservoir locations in the same region, which indicates the flood risk of a reservoir situated at a higher elevation is sensitive to the reservoir impoundment timing (e.g. shift the initial impoundment timing from September 1st to August 20th) and the reservoir water level (e.g. raise the upper boundary of the buffer pool from annual top to seasonal top). In contrast, the flood risk of a reservoir situated at a lower elevation is

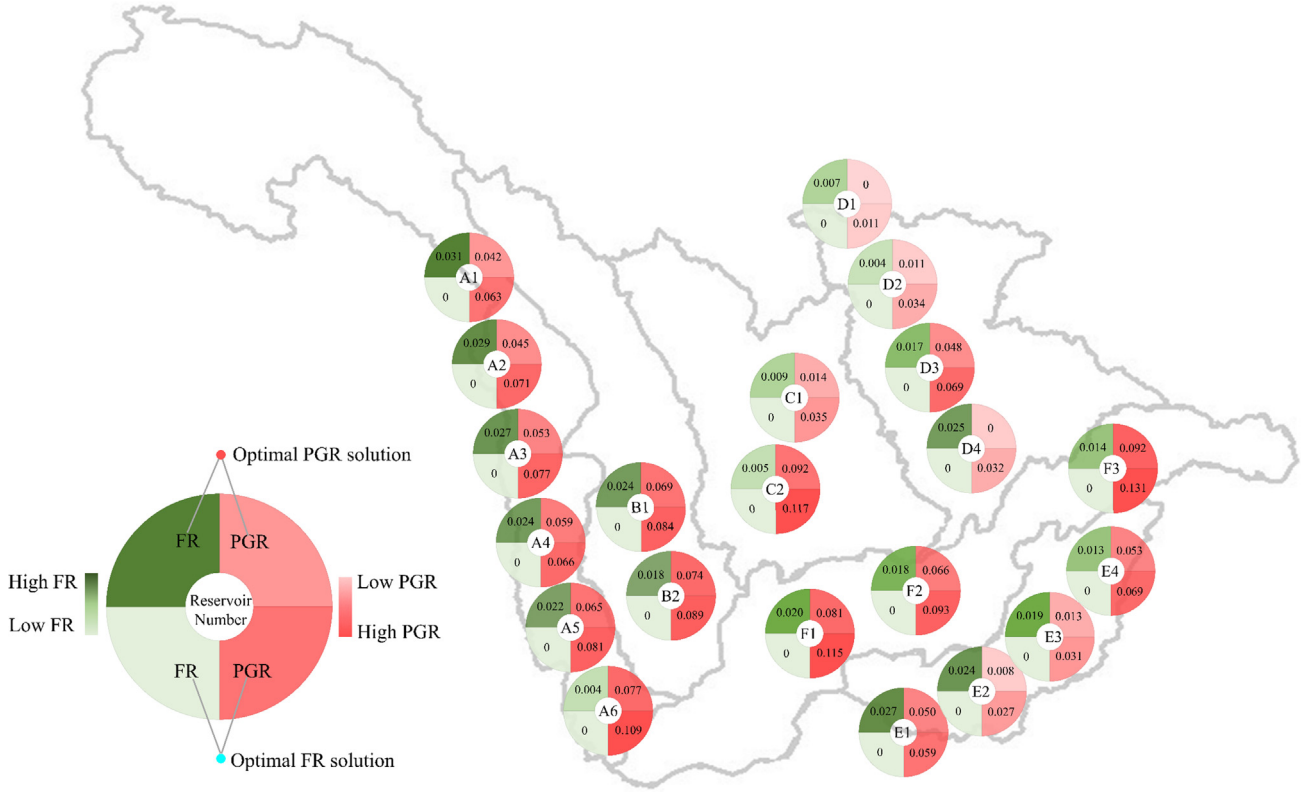

Fig. 7. Spatial distribution of FR and PGR with respect to the optimal FR and PGR solutions obtained from the NSGA-II. FR denotes flood risk. PGR denotes hydropower generation risk. The comparison is made for 21 cascade reservoirs in six regions (A-F) of the whole Upper Yangtze River Basin (WUB).

relatively insensitive to these two pre-set strategies. The reason is that along the cascade, reservoirs located at higher elevations are operated to raise reservoir water levels for increasing impoundment volumes, which result in a decrease in flood flow and the inflow of reservoirs located at lower elevations. As a consequence, the flood risk of a reservoir at a lower elevation can be significantly mitigated. The second finding is that the changes in flood risk are much larger for reservoirs with earlier initial impoundment timings than those with later impoundment timings in the same region (e.g., Reservoir A5 vs. Reservoir A6, Fig. 6). The reason is that the scales of floods occurring during earlier initial impoundment periods are commonly larger than those occurring during later impoundment periods in the same region, and thus causes higher flood risks. From Fig. 6, we notice that: (1) because Reservoir C1 is situated in parallel with Reservoir C2 and both have later initial impoundment timings (Fig. 1(b) and Table 1), there is no much difference in the maximum flood risk of the two reservoirs; and (2) along the cascade of the four reservoirs in Region D, the maximum flood risk of a reservoir with an earlier initial impoundment timing is much higher than that of a reservoir with a later initial impoundment timing in the same region (e.g., Reservoirs D3 and D4 vs. Reservoirs D1 and D2, see Table 1). Therefore, the changes in the maximum flood risk in Region D does not decrease sequentially, as compared to those of the other five regions. In Fig. 5(c), the decrease ($=PGR_{SOP} - PGR_{NSGA\text{-}II}$) of hydropower generation risk falls within 0.050 and 0.078 for the WUB. We notice that in comparison with the SOP solution, the optimal PGR solution obtained from the NSGA-II can largely improve the reliability of hydropower generation, with just a slight increase in flood risks. Besides, the changes in hydropower generation risk differ a lot among the six investigative regions, in which cascade reservoirs always suffer from different degrees (values > 0) of hydropower generation risk, except for those in Region D where the hydropower generation risks of Reservoirs D1 and D4 reach zero (Table 1 and Fig. 6). The reason is that the optimal joint operation of cascade reservoirs can easily make trade-offs between hydropower generation risk and flood risk when the installed hydropower capacity of a reservoir is small (e.g. Reservoir D1 and D4). In contrast, when the installed hydropower capacity of a reservoir is large, the hydropower generation risk cannot reduce to zero if the flood risk slightly increases (e.g. Reservoirs F1, F2 and F3, see Table 1).

4.2. Trade-offs of the risks between hydropower generation and flood control

Fig. 7 visualizes the trade-offs between flood control and hydropower generation concerning the optimal FR and PGR solutions obtained from the NSGA-II for the 21 cascade reservoirs. It is easy to identify which reservoir exposes to the maximum flood risk (e.g., the maximum value 0.031 occurs at Reservoirs A1) or the maximum hydropower generation risk (e.g., the maximum value 0.131 occurs at Reservoirs F3). According to the spatial distribution of reservoirs, the optimal PGR solution projects less flood risk on cascade reservoirs located downstream than upstream in the same region, except for Region D. The reason is that reservoirs with later initial impoundment timings will suffer lower flood risks than those with earlier timings in the same region (e.g., Reservoirs D3 and D4 vs. Reservoirs D1 and D2, see Table 1). The trade-offs between flood control and hydropower generation for each cascade reservoir revealed in Fig. 7 can significantly assist in decision-making on reservoir operation. We note that the Pareto Frontiers could help decision makers to select one of the best solutions that would satisfactorily fulfill their operation goals and benefits with the corresponding risk under a considered circumstance.

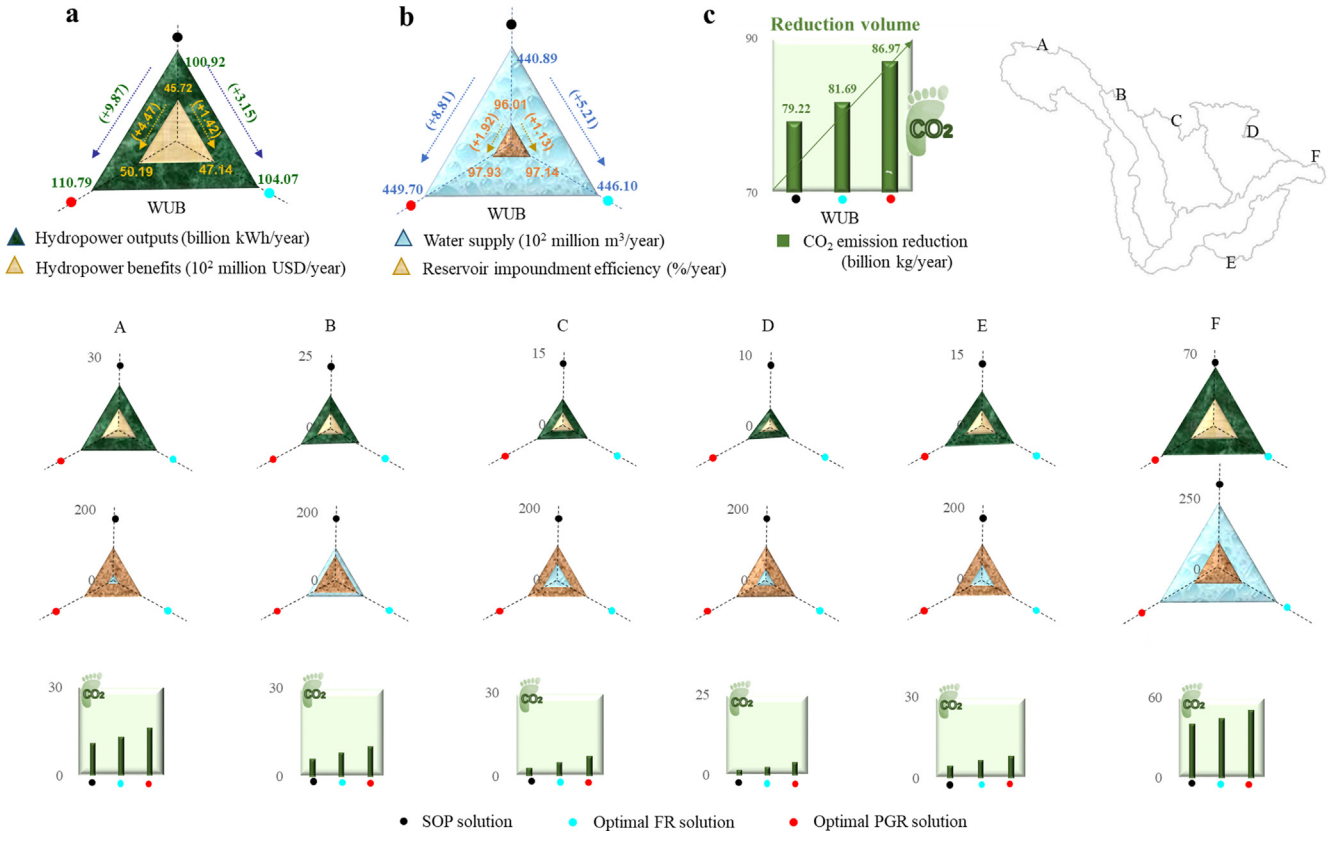

Fig. 8. Indicators of the SOP solution, the optimal flood risk (FR) solution and the optimal hydropower generation risk (PGR) solution. (a) Hydropower outputs and benefits. (b) Reservoir impoundment efficiency and water supply. (c) Reduction of CO_2 emission. The two optimal solutions were obtained from the NSGA-II. The results are presented according to the whole Upper Yangtze River Basin (WUB) and the six regions (A–F), respectively.

4.3. Hydropower benefits

The renewable hydropower energy can be fed into the power supply system of the China Power Grid to replace a part of power produced on the basis of fossil fuels. For the Upper Yangtze River Basin, the hydropower price can reach as high as 45.3 USD/MW·h. Fig. 8(a) presents the results of hydropower outputs and benefits with respect to the SOP solution, the optimal flood risk (FR) solution and the optimal hydropower generation risk (PGR) solution, respectively. It appears that the optimal FR and PGR solutions obtained from the NSGA-II model can largely improve hydropower outputs (benefits) by 3.15 billion kW·h/year (142 million USD/year) and 9.87 billion kW·h/year (447 million USD/year) accordingly. In other words, the total hydropower output can achieve 110.79 billion kW·h/year and the improvement rate of hydropower output can reach as high as 9.8%, in comparison with that of the SOP solution. The results indicate that hydropower benefits can be significantly improved when the reservoir impoundment timing can be advanced and the reservoir water level can be lifted according to the two optimal solutions. More interesting characteristics (behaviors) of the joint operation of cascade reservoirs in sub-basins (Regions A-F) can be found in this study. For example, it is noted from Fig. 8(a) that cascade reservoirs located along the mainstream (e.g. Regions A and F) produce much larger hydropower outputs and benefits than those located along tributaries (e.g. Regions B, C, D, E). This is because that reservoirs in Region A not only have higher conversion efficiency from potential energy to electricity owing to their high elevations (4000–5000 m, see Fig. 1(b)) but also has larger total installed hydropower capacity (13.76 GW, see Table 1) than the other regions. Region F produces the largest hydropower outputs and benefits out of the six regions because Region F embraces massive water, aggregated from upstream and tributaries, to generate hydropower through converting kinetic energy to electricity at high efficiency. The installed hydropower capacity of Region F reaches 44.11 GW, in which the Three Gorges Reservoir (TGR) occupies 22.50 GW.

4.4. Water utilization

Fig. 8(b) presents the results of reservoir impoundment efficiency and water supply. In comparison with the SOP solution, the optimal flood risk and hydropower generation risk solutions of the NSGA-II model can improve reservoir impoundment efficiency (water supply) by 1.13% per year (521 million m^3/year) and 1.92% per year (881 million m^3/year) accordingly. We would also like to point out that based on our proposed methodology, reservoirs with larger flood control capacities (e.g., the three reservoirs in Region F, see Table 1) will have a greater potential for significantly improving the efficiency of reservoir impoundment and water supply. With the pre-set initial impoundment timings (Table 1), we suggest that reservoirs located in the upper zone (e.g., Regions A and B) can implement reservoir impoundment operation earlier while reservoirs located in the lower zone or along the mainstream (e.g., Region F) shall implement reservoir impoundment operation later to synergistically optimize water utilization. Besides, the water supply of Regions B and F is much larger than that of the other four regions under similar reservoir impoundment rates (95–99%). This could be a consequence of the large reservoir capacities of the two regions, where the total reservoir storage capacities of Regions B and F are 13.79 billion m^3 and 62.90 billion m^3, respectively (Table 1).

4.5. CO_2 emission reduction

For China, the most suitable way to deal with the inevitable conflict between rapid economic growth and high CO_2 emission is to make a transition into a sustainable low-carbon energy system, in particular the development of renewable hydropower energy. Hydropower production cost is comparatively cheap among energy sources, and its CO_2 emission combustion is much lower than that of electricity generation from fossil fuels [42]. The GHG equivalencies calculator developed by the United States Environmental Protection Agency (https://www.epa.gov/energy/greenhouse-gas-equivalencies-calculator) was used in this study to roughly estimate the amount of CO_2 emission reduction. Considering, for example, carbon footprint values, a combined-cycle natural gas plant and a fossil energy plant have emissions of 0.350–0.400 kg and 0.800 kg CO_2 equivalent/ kW·h, respectively [42]. In contrast, a typical CO_2 emission of a hydropower plant is 0.015 kg CO_2 equivalent/ kW·h, which is about 30–60 times less than those of fossil fuel generation [4]. Thus, the CO_2 emission reduction for hydropower production in comparison with fossil energy is equal to 0.785 kg CO_2 equivalent/kWh (CO_2 equivalent of fossil energy − CO_2 equivalent of hydropower = 0.800 − 0.015). Fig. 8(c) presents the CO_2 emission reduction, and the results of the optimal flood risk solution and the optimal hydropower generation risk solution indicate that the CO_2 emission can be reduced by 2.47 billion kg/year and 7.75 billion kg/year, respectively for the WUB, in comparison with the SOP solution. Such huge reduction of CO_2 emission can be achieved and will make a great contribution to improving air quality and eco-environment locally if the renewable hydropower can be implemented to replace the thermal power. It is also noted that the reduction of CO_2 emission in Regions A and F is obviously much more significant than that of the other four regions. Taking account of the hydropower outputs shown in Fig. 8(a), it reveals that the higher the hydropower output is, the more the CO_2 emission can be reduced. This is because the reduced volume of CO_2 emission is linearly dependent on hydropower output through the GHG equivalencies calculator (i.e., 0.785 kg/kWh).

5. Conclusions

Encountering great challenges and dilemmas in energy production and CO_2 emission mitigation, China nowadays is in transition to a low-carbon and renewable energy system for sustainable development. Hydroelectricity is expected to trigger greater development in the future and contribute significantly to the low-carbon economy. The joint operation of reservoirs can better utilize water resources, however, difficulty faced in joint operation soars quickly as the number of reservoirs increases. In this study, we aim at maximizing the hydropower output of 21 mega cascade reservoirs (storage capacity ≥200 million m^3) in the Upper Yangtze River Basin of China during flood seasons. The proposed methodology integrated the Non-Dominated Sorting Genetic Algorithm-II (NSGA-II) with a successive approximation approach based on two designed impoundment strategies to synergistically optimize the multi-objectives of 21 jointed cascade reservoirs operation. The successive approximation approach could effectively decompose the mutually related M-dimensional problem into M individual one-dimensional problems, which would ingeniously overcome the curse of dimensionality. The results demonstrated that our proposed methodology not only could significantly increase the efficiency and benefits of hydropower generation (reaching 110.79 billion kW·h/year, i.e. 9.8% improvement, as compared with 21 single reservoir operation using the SOP) but also could greatly contribute to water utilization and CO_2 emission reduction with a very small flood risk (less than 0.016). Consequently, a new niche of joint cascade reservoir operation can be explored to lift hydropower output at no or little cost of flood risk, accompanied with benefits in water supply and CO_2 emission reduction. In accordance with the Pareto Frontiers obtained from the NSGA-II, we also suggest operational guidelines for decision makers and stakeholders to implement adequate reservoir operation according to the magnitudes of flood events. From the technical point of view, the main differences between the SOP solution and the NSGA-II optimal solutions are: (1) the former is a conventional simulation method while the latter is a multi-objective optimization algorithm by a powerful state-of-the-art tool (an AI technique); (2) the former produces linear operation while the latter produces non-linear

operation; and (3) the former considers only one objective at a time and thus fails to synergistically optimize two objectives simultaneously while the latter not only provides the best solution for each objective but supplies a large number of optimal solutions (1000 in our case) for both objectives, which could help decision makers to choose one of the best solutions to fulfill their goals with corresponding risk under a considered circumstance.

For future work in making real-time joint operation of cascade reservoirs in response to a foreseeable flood event in a vast watershed, we suggest to explore a real-time optimal reservoir operation methodology that maximizes the hydropower generation and water utilization under the limitation of no flood risk. Accurate and reliable multi-step-ahead forecasts on the arrival and the peak of a flood using modern techniques like AI and remote sensing [20,43,44] will substantially assist decision makes in precisely determining which optimal solution is appropriate to implement for curtailing the risks in flood control and hydropower generation.

Acknowledgments

This study was financially supported by the National Key Research and Development Project of China (Grant No. 2016YFC0402206), the National Natural Science Foundation of China (Grant No. 51509008 and 51422907) and the Ministry of Science and Technology, Taiwan, ROC (MOST 105-2811-B-002-151; MOST 106-2627-M-002-025). The authors would like to thank the editors and anonymous reviewers for their valuable and constructive comments related to this manuscript.

References

[1] Guan D, Meng J, Hubacek K, Song M, Wei YM, Shan Y, et al. Chinese CO_2 emission flows have reversed since the global financial crisis. Nat Commun 2017;8:1712–21. https://doi.org/10.1038/s41467-017-01820-w.
[2] UNEP. The emissions gap report. United Nations Environment Programme; 2016.
[3] NBSC. China statistical yearbook. National Bureau of Statistics of China; 2016.
[4] Ming B, Liu P, Guo S, Zhang X, Feng M, Wang X. Optimizing utility-scale photovoltaic power generation for integration into a hydropower reservoir by incorporating long- and short-term operational decisions. Appl Energy 2017;204:432–45. https://doi.org/10.1016/j.apenergy.2017.07.046.
[5] Lu D, Wang B, Wang Y, Zhou H, Liang Q, Peng Y, et al. Optimal operation of cascade hydropower stations using hydrogen as storage medium. Appl Energy 2015;137:56–63. https://doi.org/10.1016/j.apenergy.2014.09.092.
[6] Kan G, Zhang M, Liang K, Wang H, Jiang Y, Li J, et al. Improving water quantity simulation & forecasting to solve the energy-water-food nexus issue by using heterogeneous computing accelerated global optimization method. Appl Energy 2016;210:420–33. https://doi.org/10.1016/j.apenergy.2016.08.017.
[7] Qi Y, Stern N, Wu T, Lu J, Green F. China's post-coal growth. Nat Geosci 2016;9:564–6.
[8] Balkhair KS, Rahman KU. Sustainable and economical small-scale and low-head hydropower generation: a promising alternative potential solution for energy generation at local and regional scale. Appl Energy 2017;188:378–91. https://doi.org/10.1016/j.apenergy.2016.12.012.
[9] Vliet MTHV, Wiberg D, Leduc S, Riahi K. Power-generation system vulnerability and adaptation to changes in climate and water resources. Nat Clim Change 2016;6:375–81. https://doi.org/10.1038/NCLIMATE2903.
[10] Gebretsadik Y, Fant C, Strzepek K, Arndt C. Optimized reservoir operation model of regional wind and hydro power integration case study: Zambezi basin and South Africa. Appl Energy 2016;161:574–82. https://doi.org/10.1016/j.apenergy.2015.09.077.
[11] Li B, et al. The contribution of China's emissions to global climate forcing. Nature 2016;531:357–62. https://doi.org/10.1038/nature17165.
[12] Boehlert B, Strzepek KM, Gebretsadik Y, Swanson R, Mccluskey A, Neumann JE, et al. Climate change impacts and greenhouse gas mitigation effects on U.S. hydropower generation. Appl Energy 2016;183:1511–9. https://doi.org/10.1016/j.apenergy.2016.09.054.
[13] Korsbakken JI, Peters GP, Andrew RM. Uncertainties around reductions in China's coal use and CO_2 emissions. Nat Clim Change 2016;6:687–90. https://doi.org/10.1038/NCLIMATE2963.
[14] Hu Y, Cheng H. The urgency of assessing the greenhouse gas budgets of hydroelectric reservoirs in China. Nat Clim Change 2013;3:708–12. https://doi.org/10.1038/NCLIMATE1831.
[15] Li X, Chen Z, Fan X, Cheng Z. Hydropower development situation and prospects in China. Energy 2018;82:232–9. https://doi.org/10.1016/j.rser.2017.08.090.
[16] Zhang L, Sovacool BK, Ren J, Ely A. The Dragon awakens: innovation, competition, and transition in the energy strategy of the People's Republic of China, 1949–2017. Energy Policy 2017;108:634–44. https://doi.org/10.1016/j.enpol.2017.06.027.
[17] Li Y, Li Y, Ji P, Yang J. The status quo analysis and policy suggestions on promoting China's hydropower development. Renew Sustain Energy Rev 2015;51:1071–9. https://doi.org/10.1016/j.rser.2015.07.044.
[18] Chang-Jiang Water Resources Commission (CWRC).. Chang-Jiang and Southwest rivers water resources bulletin in 2016. Chang-Jiang Press; 2017. [in Chinese].
[19] Li FF, Qiu J. Multi-objective optimization for integrated hydro–photovoltaic power system. Appl Energy 2016;167:377–84. https://doi.org/10.1016/j.apenergy.2015.09.018.
[20] Demissie AA, Solomon AA. Power system sensitivity to extreme hydrological conditions as studied using an integrated reservoir and power system dispatch model, the case of Ethiopia. Appl Energy 2016;182:442–63. https://doi.org/10.1016/j.apenergy.2016.08.106.
[21] Jurasz J, Ciapała B. Integrating photovoltaics into energy systems by using a run-off-river power plant with pondage to smooth energy exchange with the power gird. Appl Energy 2017;198:21–35. https://doi.org/10.1016/j.apenergy.2017.04.042.
[22] Cheng CT, Shen JJ, Wu XY, Chau KW. Operation challenges for fast-growing China's hydropower systems and respondence to energy saving and emission reduction. Renew Sustain Energy Rev 2012;16:2386–93. https://doi.org/10.1016/j.rser.2012.01.056.
[23] Heidari M, Chow VT, Kokotović PV, Meredith DD. Discrete differential dynamic programing approach to water resources systems optimization. Water Resour Res 1971;7(2):273–82. https://doi.org/10.1029/WR007i002p00273.
[24] Turgeon A. Optimal short-term hydro scheduling from the principle of progressive optimality. Water Resour Res 1981;17(3):481–6. https://doi.org/10.1029/WR017i003p00481.
[25] Howson HR, Sancho NGF. A new algorithm for the solution of multi-state dynamic programming problems. Math Program 1975;8(1):104–16. https://doi.org/10.1007/BF01580431.
[26] Larson RE, Korsak AJ. A dynamic programming successive approximations technique with convergence proofs. Automatica 1970;6(2):245–52. https://doi.org/10.1016/0005-1098(70), 90095-6.
[27] Kumar ND, Reddy JM. Multipurpose reservoir operation using particle swarm optimization. J Water Resour Plann Manage 2007;133(3):192–201. https://doi.org/10.1061/(ASCE)0733-9496.
[28] Ehteram M, Allawi MF, Karami H, Mousavi SF, Emami M, Ahmed ES, et al. Optimization of chain-reservoirs' operation with a new approach in artificial intelligence. Water Resour Manage 2017;31(7):2085–104. https://doi.org/10.1007/s11269-017-1625-6.
[29] Singh VK, Singal SK. Operation of hydro power plants-a review. Renew Sustain Energy Rev 2017;69:610–9. https://doi.org/10.1016/j.rser.2016.11.169.
[30] Chang LC, Chang FJ. Multi-objective evolutionary algorithm for operating parallel reservoir system. J Hydrol 2009;377:12–20. https://doi.org/10.1016/j.jhydrol.2009.07.061.
[31] Ahmadi M, Haddad OB, Mariño MA. Extraction of flexible multi-objective real-time reservoir operation rules. Water Resour Manage 2014;28(1):131–47. https://doi.org/10.1007/s11269-013-0476-z.
[32] Jia B, Simonovic SP, Zhong P, Yu Z. A multi-objective best compromise decision model for real-time flood mitigation operations of multi-reservoir system. Water Resour Manage 2016;30(10):3363–87. https://doi.org/10.1007/s11269-016-1356-0.
[33] Wan W, Guo X, Lei X, Jiang Y, Wang H. A novel optimization method for multi-reservoir operation policy derivation in complex inter-basin water transfer system. Water Resour Manage 2018;1–21. https://doi.org/10.1007/s11269-017-1735-1.
[34] Deb K, Pratap A, Agarwal S, Meyarivan T. A fast and elitist multiobjective genetic algorithm: NSGA-II. IEEE Trans Evol Comput 2002;6:182–97. https://doi.org/10.1109/4235.996017.
[35] Choong SM, El-Shafie A. State-of-the-art for modelling reservoir inflows and management optimization. Water Resour Manage 2015;29(4):1267–82. https://doi.org/10.1007/s11269-014-0872-z.
[36] Zhou Y, Guo S, Xu CY, Liu P, Qin H. Deriving joint optimal refill rules for cascade reservoirs with multi-objective evaluation. J Hydrol 2015;524:166–81. https://doi.org/10.1016/j.jhydrol.2015.02.034.
[37] Chang FJ, Wang YC, Tsai WP. Modelling intelligent water resources allocation for multi-users. Water Resour Manage 2016;30:1395–413. https://doi.org/10.1007/s11269-016-1229-6.
[38] Haghighi A, Asl AZ. Uncertainty analysis of water supply networks using the fuzzy set theory and NSGA-II. Eng Appl Artif Intell 2014;32:270–82. https://doi.org/10.1016/j.engappai.2014.02.010.
[39] Tsai WP, Chang FJ, Chang LC, Herricks EE. AI techniques for optimizing multi-objective reservoir operation upon human and riverine ecosystem demands. J Hydrol 2015;530:634–44. https://doi.org/10.1016/j.jhydrol.2015.10.024.
[40] Zhou Y, Guo S, Chang F, Liu Pan, Chen AB. Methodology that improves water utilization and hydropower generation without increasing flood risk in mega cascade reservoirs. Energy 2018;143:785–96. https://doi.org/10.1016/j.energy.2017.11.035.
[41] Lotfan S, Akbarpour Ghiasi R, Fallah M, Sadeghi MH. ANN-based modeling and reducing dual-fuel engine's challenging emissions by multi-objective evolutionary algorithm NSGA-II. Appl Energy 2016;175:91–9. https://doi.org/10.1016/j.apenergy.2016.04.099.
[42] EPA. AVERT, U.S. national weighted average CO_2 marginal emission rate, year 2016 data. Washington, DC: U.S. Environmental Protection Agency; 2017.
[43] Chang FJ, Tsai MJ. A nonlinear spatio-temporal lumping of radar rainfall for modelling multi-step-ahead inflow forecasts by data-driven techniques. J Hydrol 2016;535:256–69. https://doi.org/10.1016/j.jhydrol.2016.01.056.
[44] Chang LC, Chen PA, Chang FJ. Reinforced two-step-ahead weight adjustment technique for online training of recurrent neural networks. IEEE Trans Neural Networks Learn Syst 2012;23:1269–78. https://doi.org/10.1109/TNNLS.2012.2200695.